



Variation characteristics of sporadic-E layer in East Asia

based on long-term data

**Hai-Sheng Zhao¹, Jie Feng^{* 2}, Yang Liu², Zheng-Wen Xu², Jian Wu³, Kun Xue²,
Huai-Yun Peng², Zing-Hua Ding³**

¹ School of Electronic Science and Technology, Hainan University, Haikou 570228, China

² National Key Laboratory of Electromagnetic Environment, China Research Institute of Radiowave
Propagation, Qingdao 266107, China

³ Kunming Electro-Magnetic Environment National Observation and Research Station, China
Research Institute of Radiowave Propagation, Qijing 655500, China.

* Correspondence: fengjie@crip.ac.cn

Abstract: The characteristics of ionospheric intensity, spatial distribution, diurnal variation, seasonal variation and long-term variation in East Asia are studied by using the ionospheric observation data from 21 ionosonde stations in China and Japan over the past 60 years. It is found that the Es layer intensity in East Asia is much higher than the global average, and the intensity center is located near the 30° N line, and weakens to low and high latitudes. At the same time, the intensity center of Es layer is not fixed, and the intensity center migrates with diurnal and seasonal variations. The regions with stronger Es showed a long-term downward trend, while the regions with weaker Es showed a long-term upward trend in East Asia.

Key words East Asia, Sporadic E Layer, Variation Characteristics, Long-term Trend, Spatial Distribution

1 Introduction

Sporadic E (Es) is a transient electron density enhancement structure that occurs at altitude of 90-140 kilometers and can significantly affect the propagation of radio waves. The Es layer may occur during the day or at night, and its variations with latitude and time are pronounced." The Es layer is a special structure within the ionosphere, unlike the regular E layer that exhibits stable and regular morphological structures and trends. Instead, it is a transient and irregular strong ionization layer, with a height range of 90 to 140 km and a thickness ranging from a few hundred meters to 1 km [Danilov et al., 2020; Pignalberi et al., 2014]. Its horizontal scale varies from tens of kilometers to hundreds of kilometers, and it drifts at speeds ranging from 20 to 300 m/s [Maeda et al., 2016]. The seasonal distribution of the Es layer in the ionosphere is uneven, with higher occurrence frequencies in summer months from May to August and lower frequencies in other



months [Sivakandan et al., 2023; Jacobi et al., 2019; Haldoupis et al., 2007]. The Es layer in the ionosphere exhibits significant diurnal variation, with higher occurrence frequencies during the day and lower frequencies during the night. The electron density in the Es layer of the ionosphere is exceptionally high, reaching up to 100 times the electron density of the regular E layer. Therefore, the Es layer in the ionosphere is capable of reflecting radio waves that would otherwise penetrate through to the F layer, resulting in the reflection and scattering of HF/VHF frequency radio waves. The maximum single-hop propagation distance can exceed 2000 km.

In the early 20th century, unexpected reflected signals received by instruments such as altimeters, television, and amplitude-modulated radios sparked great interest among researchers [Whitehead, 1970, 1989], leading to the beginning of studies on the Es layer of the ionosphere. Since the 1960s, scientists have gradually gained understanding of the Es layer and its related characteristics through observations and analysis using instruments such as ionospheric sounders [Whitehead, 1970, 1989; Reddy et al., 1968], incoherent scatter radars [Swartz et al., 1974; Ioannidis et al., 1972], sounding rockets [Yamamoto et al., 1998; Pfaff et al., 1998; Kelley et al., 1995; Smith, 1970; Seddon et al., 1962], coherent scatter radars, and other methods [Haldoupis et al., 1996, 1997]. They have established and continuously improved theories on the formation mechanism of the Es layer in the ionosphere, and have gradually acquired knowledge about its radio wave propagation characteristics. The wind shear theory is considered to be the primary mechanism for the formation of the mid-latitude Es layer [Axford et al., 1963; Didebulidze et al., 2015]. Under the influence of the geomagnetic field, the horizontal wind generates vertical shear force on ions at the height of the ionospheric dynamo layer, compressing the ion constituents and forming a thin layer of high-density ionization, namely the Es layer. Tidal waves, planetary waves, and gravity waves affect the wind shear, causing metallic ions and molecular ions to move and converge, forming thin high-density plasma layers in mid-latitudes [Qiu et al., 2023; Haldoupis et al., 2006; Axford et al., 1966; Helmboldt et al., 2016; Christos et al., 2004, 2006; Davis et al., 2006; Tepley et al., 1985; Macleod et al., 1975]. Although the wind shear theory is currently the mainstream explanation for the formation of the Es layer, the theory itself is still not fully developed [Liu et al., 2022], and there are still difficulties in explaining certain phenomena, such as the summer anomalies of the mid-latitude Es layer and the extremely uneven distribution of Es layer intensity globally.

The unpredictability and highly uneven spatial-temporal distribution of the Es layer have sparked great interest among researchers, initiating relentless studies for over half a century. In the 1950s, Smith [Smith et al., 1957] proposed the concept of the "Far East Anomaly" based on statistical analysis of global vertical sounding records and research on VHF over-the-horizon propagation phenomena. The Far East Anomaly refers to the phenomenon where the occurrence



70 rate and intensity of Es layers in the mid-latitude regions of the Far East are exceptionally high far
71 exceeding those in other regions at the same latitude. Correspondingly, during the summer in the
72 southern hemisphere, the Es layer in the South American region is also relatively strong with a
73 higher occurrence rate, but it is not as prominent as the Far East Anomaly. With the development
74 of satellite technology, the method of detecting the spatial distribution of the Es layer using
75 satellite beacons has gradually matured. The distribution of the global Es layer has been obtained
76 based on GPS radio occultation technique [Arras et al., 2009], which has greatly expanded the
77 research methods for the Es layer and has epoch-making significance. Due to the scarcity of early
78 ionosonde stations for the Es layer and insufficient data accumulation, early studies on the
79 morphology of the Es layer could only provide a rough global distribution of the Es layer. The
80 radio occultation observations also has its limitations, such as it cannot continuously observe the
81 Es layer at fixed location compared to the ground-based observations. It can only estimate Es layer
82 intensity through phase and amplitude variations, and its accuracy needs to be improved.

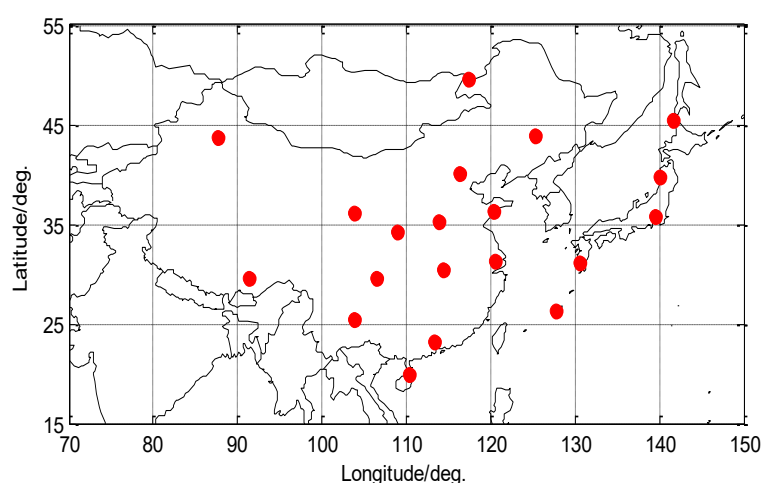
83 With the increasing number of global ionosonde stations and the accumulation of data over
84 time, conducting long-term studies on the Es layer's characteristics using global ionosonde data is
85 of significant scientific importance. Eastern Asia is located in the peak region of the Far East
86 Anomaly, making it uniquely advantageous for research. In this study, utilizing over 60 years of
87 Es layer observation data from 21 ionosonde stations in China and Japan [Zhao, 2024a], we
88 conducted in-depth research on the intensity characteristics, spatial distribution, diurnal variation,
89 seasonal variation, and long-term variations of the Es layer in the Eastern Asian. The data analysis
90 software on which this article is based are available in Zhao. [2024b]. The research findings of this
91 study are of great significance for exploring the formation mechanisms of the Es layer, analyzing
92 the spatial-temporal distribution and long-term trends of Es layer intensity. Additionally, the Es
93 layer exhibits high scattering efficiency for VHF frequency signals and has advantages in VHF
94 over-the-horizon propagation. This makes it valuable for achieving long-distance, sudden
95 communication and meeting the minimum requirements for information transmission.

96 2 Ionosonde Station Network and Data Sources in China and Japan

97 Ground-based radio vertical sounding of the ionosphere is one of the fundamental methods
98 for ionospheric exploration and was the only effective means of investigation before the advent of
99 rockets and artificial satellites. After years of development, the network of ionosonde stations in
100 China has gradually covered a vast area of our country, spanning 30 degrees in geomagnetic
101 latitude and longitude. The longitude intervals are between 3 to 10 degrees, while the latitude
102 intervals range from 3 to 6 degrees. Particularly, in the geomagnetic sector of 180 to 193 degrees



103 east, a meridional chain of six stations has been established, forming a well-designed network of
104 ionosonde stations that meets the needs of shortwave communication frequency prediction and
105 related radio wave propagation studies. Currently, through the joint efforts of various universities
106 and research institutions in China, significant achievements have been made in the field of
107 ionospheric exploration. These include shortwave communication frequency prediction,
108 ionospheric disturbance forecasting, and the refractive correction for tracking and locating rocket
109 experiments.



110

111

Fig.1 ionosonde stations in China and Japan

112

113

114

115

116

117

118

The Es data primarily comes from ionosonde stations in China, including Beijing, Changchun, Chongqing, Guangzhou, Hainan, Lhasa, Manzhouli, Urumqi, Wuhan, Xinxiang, Kunming, Qingdao, Suzhou, Sheshan, Xi'an, as well as surrounding areas in China. Additionally, data from the OKINAWA (Okinawa Island, Japan), YAMAGAWA (Yamagawa Prefecture, Japan), Koku, Akita, and Wakkanai ionosonde stations are also included, as shown in Figure 1. The names, nationalities, coordinates, and data periods of each stations are list in Table 1.

Table 1 the observation stations and terms of Es

Index	Station name	Country	Longitude	Latitude	Time period
1	Beijing	China	N40.11°	E116.27°	1958~2020
2	Changchun	China	N43.84°	E125.27°	1957~2020
3	Chongqing	China	N29.50°	E106.40°	1958~2020
4	Guangzhou	China	N23.15°	E113.35°	1958~2020
5	Haikou	China	N20.00°	E110.33°	1958~2020
6	Lanzhou	China	N36.06°	E103.87°	1958~2020
7	Lhasa	China	N29.63°	E91.28°	1970~2020
8	Manzhouli	China	N49.58°	E117.45°	1958~2020
9	Urumchi	China	N43.75°	E87.63°	1958~2020
10	Qingdao	China	N36.24°	E120.41	2000~2020
11	Sheshan	China	N31.00°	E121.24°	1961~1966
12	Kunming	China	N 25.50°	E103.80°	2007~2020

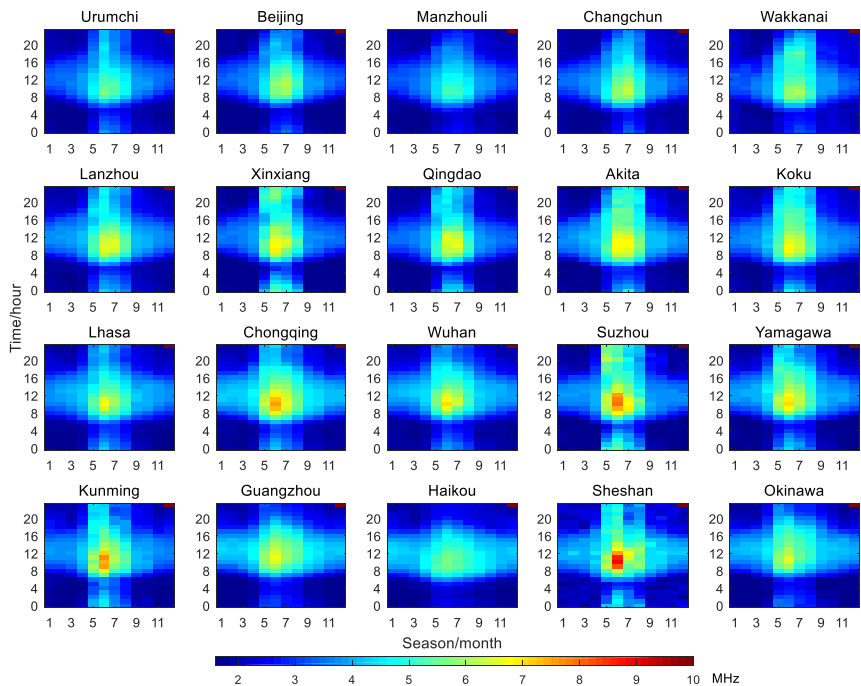


13	Xinxiang	China	N35.30°	E113.95°	2008~2020
14	Suzhou	China	N31.30°	E120.65°	2008~2020
15	Xian	China	N34.23°	E108.92°	2011~2020
16	Wuhan	China	N30.50°	E114.40°	1957~1998
17	Akita	Japan	N39.70°	E140.10°	1965~1993
18	Okinawa	Japan	N26.30°	E127.80°	1972~2010
19	Yamagawa	Japan	N31.20°	E130.60°	1965~2010
20	Wakkanai	Japan	N45.40°	E141.70°	1957~2005
21	Koku	Japan	N35.70°	E139.50°	1958~2005

119

120 3 Characteristics of Es layer intensity in East Asia

121 The monthly median of the Es layer critical frequency (foEs) is an important parameter for
122 assessing the Es layer intensity in a specific region. The foEs monthly median reflects the average
123 level of the Es layer intensity in that region and possesses a high level of reliability. Figure 2
124 presents the variations of the monthly median foEs with local time and month for 20 stations in
125 East Asia.



126

127 Fig.2 local time-month distributions of foEs monthly median located at different stations

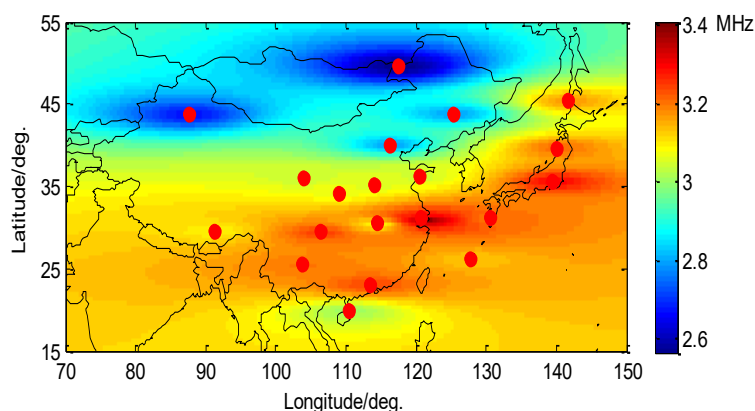
128 According to figure 2, the foEs layer intensity during the summer months (May to August) is
129 significantly higher than in other seasons. The foEs layer intensity is also notably higher around



130 local noon compared to other times of the day. Additionally, the Es layer intensity in East Asia
131 exhibits a strong spatial non-uniformity. Generally, the distribution of Es layer intensity centers
132 around the latitude of 30 degrees north, decreasing towards lower and higher latitudes. The overall
133 intensity is higher at lower latitudes compared to higher latitudes, and the intensity is slightly
134 stronger in the eastern region compared to the western region. The maximum monthly average
135 foEs values for all stations are above 5 MHz, with some stations reaching even higher values
136 exceeding 9 MHz, which is significantly higher than the global average level [Smith et al., 1970].

137 4 Spatial distribution characteristics of Es layer in East Asia

138 The spatial distribution of foEs is crucial for investigating the characteristics of the Es layer
139 in a specific region. In this section, the distribution of the annual mean value of foEs in East Asia
140 is given by the Kriging interpolation method [Zhu et al., 20223; Liu et al., 2022] based on the
141 annual mean value of foEs at each station (as shown in figure 3).



142
143 Fig.3 the distribution of foEs average values in East Asia

144 From Figure 3, it is shown that the Es layer intensity in East Asia exhibits a zonal distribution
145 along the latitude. The peak intensity of foEs occurs near 30 degrees north latitude. Over the years,
146 there has been ongoing debate regarding the center of global Es layer intensity. Some researchers
147 argue that the center of global Es layer intensity is near Wakkanai, Japan [Smith et al., 1970].
148 However, figure 3 clearly shows that while the average Es layer intensity in the sea area near
149 Wakkanai, Japan is relatively high, it is not the area with the highest intensity of Es layer. The
150 actual center of Es layer intensity should be located near Suzhou, China. Rather than considering
151 the Es layer intensity center as a single point, it is more appropriate to view it as a zonal region,
152 with the center of this region lying along the 30 degrees north latitude line.



5 Temporal distribution characteristics of Es layer in East Asia

5. 1 Diurnal variation characteristics

In order to further investigate the diurnal variation patterns of Es layer intensity in East Asia, the study presents the average variations of monthly median foEs values with time. Due to the large number of stations, five representative stations near 30 degrees north latitude, namely Lhasa, Chongqing, Wuhan, Suzhou, and Yamagawa, as well as six representative stations near 120 degrees east longitude, namely Manzhouli, Changchun, Qingdao, Suzhou, Guangzhou, and Haikou, were selected. The diurnal variation curves for each of these stations are provided in figure 4.

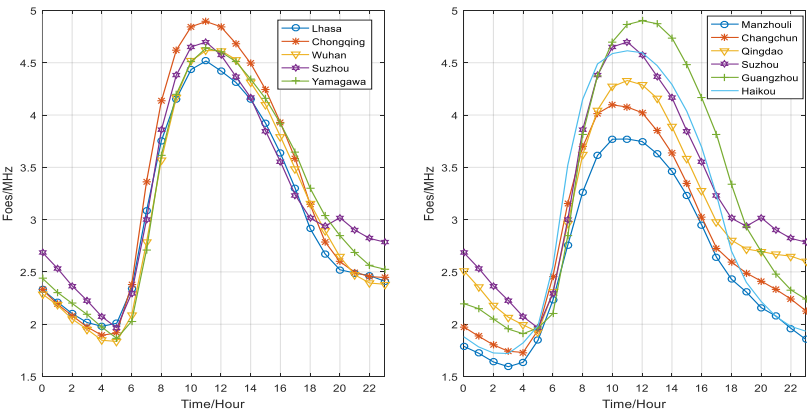


Fig.4 Diurnal variation curves of foEs monthly median

From figure 4, it is shown that the maximum values of foEs in East Asia generally occur around 11 AM, while the minimum values typically occur around 5 AM. At daytime, foEs values are significantly higher than during the nighttime.

To further investigate the diurnal variation characteristics of Es layer intensity in East Asia, figure 5 presents the spatial distribution characteristics of foEs monthly median values during daytime and nighttime. (Daytime is defined as 8 AM to 5 PM, and nighttime is defined as 9 PM to 6 AM the following day).

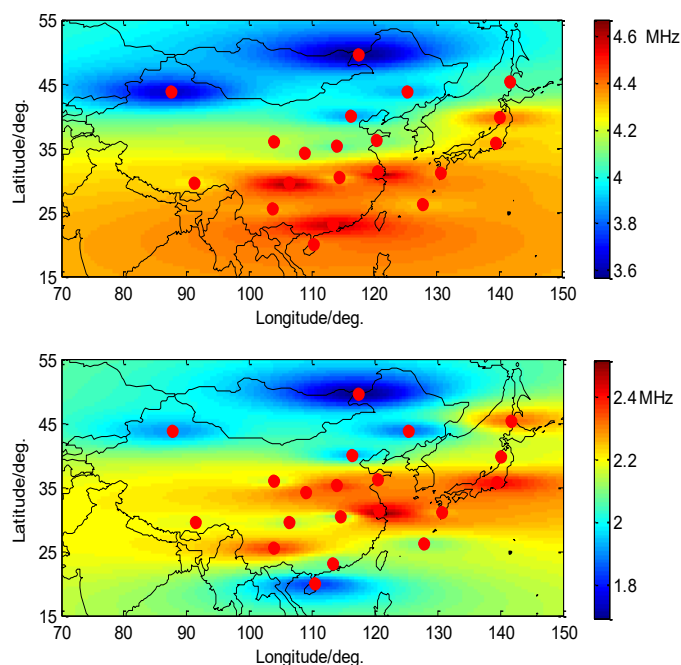


Fig.5 the day and night comparison of foEs average values

Figure 5 shows that at daytime, the center of Es layer intensity in East Asia is located in areas such as Chongqing, Guangzhou, and Suzhou in China. During the nighttime, the center of Es layer intensity migrates towards the northeast, with the strongest area appearing in regions such as Suzhou and Qingdao in China, as well as Koku and Yamagawa in Japan. The diurnal drift in the center of Es layer may be affected by environmental factors such as the diurnal variations of background atmosphere and climate.

5. 2 Seasonal variation characteristics

To further investigate the seasonal variation characteristics of the Es layer in East Asia, figure 6 presents the average variations of monthly median foEs values with seasons. The station selection is the same as in section 5.1.

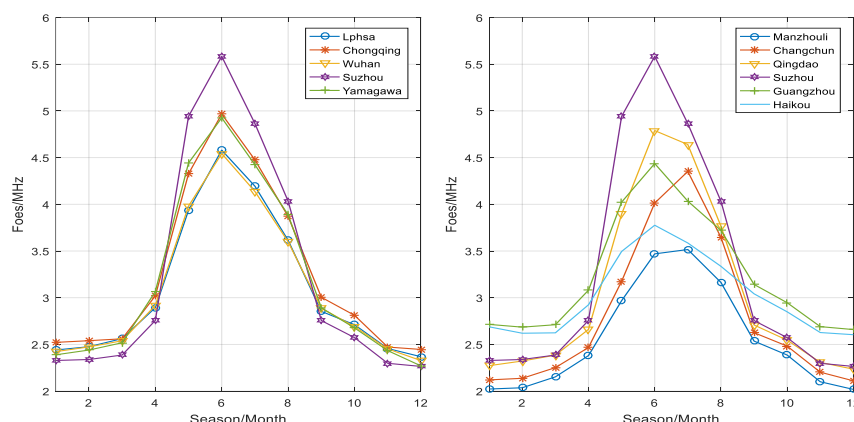


Fig.6 seasonal variation curves of foEs average values

According to figure 6, the maximum values of foEs in East Asia generally occur in June, while the minimum values typically occur in December. The foEs values in summer are significantly higher than in winter.

To further investigate the seasonal variation characteristics of Es layer intensity in East Asia, figure 7 presents the spatial distribution characteristics of the average monthly median foEs values during summer and winter. (Summer is defined as May to August, and winter is defined as November to February of the following year).

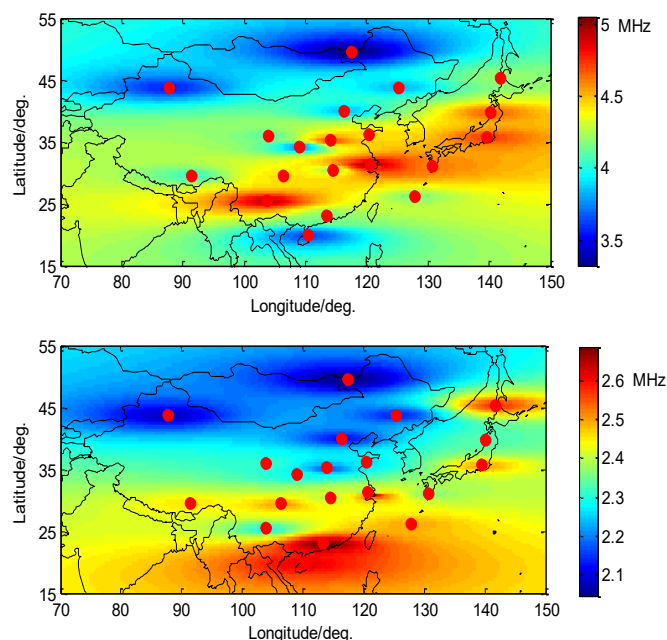


Fig.7 the summer and winter comparison of foEs average values



Figure 7 shows that during the summer in East Asia, the center of Es layer intensity is located near 30 degrees north latitude, exhibiting a zonal distribution. However, during the winter, the center of Es layer intensity migrates southward towards the Guangzhou and Haikou.

The proposal of the wind shear theory and the discovery of metallic ions provide a reasonable explanation for the formation process of the Es layer. Measurements of ion density and wind velocity through rocket experiments have confirmed the fundamental concept of wind shear compression. However, the occurrence of anomalous phenomena in the mid-latitude Es layer during summer poses a challenge to the wind shear theory. In order to address this issue, some scholars have conducted in-depth research by linking the occurrence rate of mid-latitude Es layer with planetary waves. They propose that planetary waves are also an important factor influencing the mid-latitude Es layer and suggest that the viewpoint of planetary waves can provide a reasonable explanation for the summer anomaly phenomenon. Furthermore, they indicate that planetary waves modulate tidal amplitudes, load information onto tides, and indirectly affect the Es layer through tides. They also predict that the modulation of tides by planetary waves is achieved through nonlinear interference [Xu et al., 2022].

From the analysis of the probability distribution, intensity distribution, diurnal variation, and seasonal variation of the Es layer, we have observed a general pattern: the center of Es layer intensity seems to be chasing the center of high temperatures in the lower atmosphere. Regions with higher average temperatures tend to exhibit stronger Es layer intensity, whereas regions with lower temperatures tend to have weaker Es layer intensity. The strong correlation between Es layer intensity and lower atmospheric temperature may be attributed to the influence of temperature variations in the lower atmosphere [Zhao et al., 2024], which drive atmospheric motion and generate atmospheric waves. Additionally, more intense atmospheric waves are generated when the lower atmospheric temperature is higher. These waves gradually propagate from the lower atmosphere to the height of the Es layer, affecting the formation process of the Es layer. As a result, the Es layer intensity shows a high consistency with the surface atmospheric temperature. We will conduct targeted research to further investigate the correlation between Es layer intensity and surface temperature.

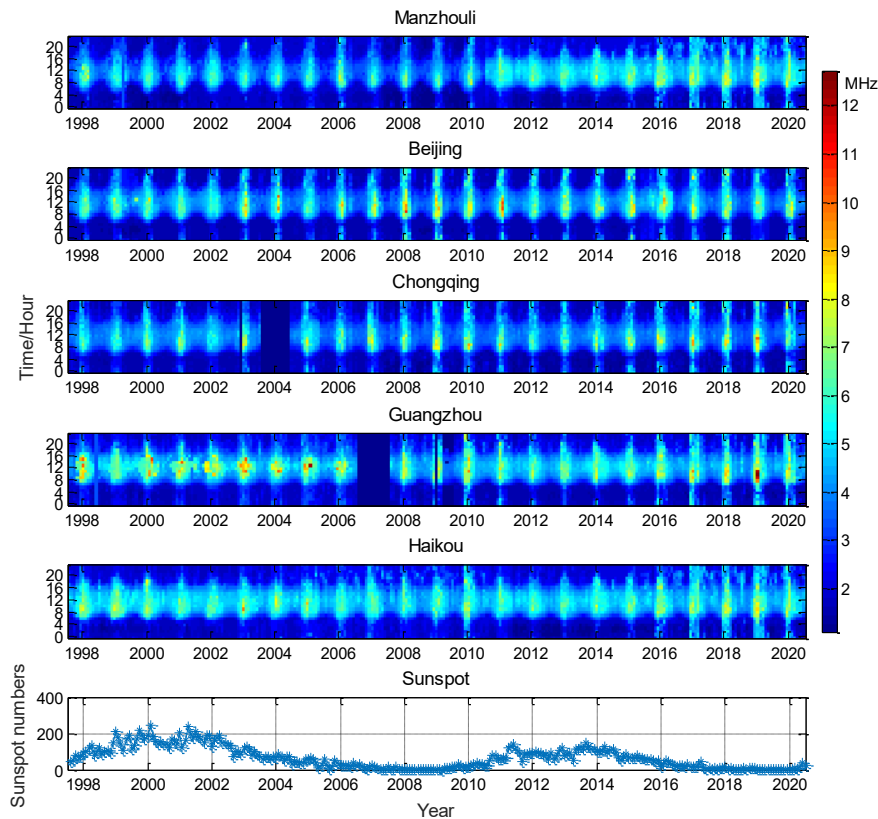
5. 3 Solar cycle variation characteristics

The correlation between Es layer intensity and solar cycles has been a focal point of debate in the scientific community. Different scholars have drawn contradictory conclusions, including positive correlation, negative correlation, and no correlation, based on observations from different stations [Tan et al., 1985; Maksyutin et al., 2005; Closs et al., 1965; Zuo et al., 2006]. Currently, there are three main viewpoints. One viewpoint suggests that Es layer intensity is independent of



228 solar activity, implying no significant influence. Another perspective proposes a weak positive
229 correlation between Es layer intensity and solar activity, implying that variations in solar cycles
230 may have a slight impact on Es layer intensity. In contrast, there is a third viewpoint suggesting a
231 weak negative correlation between Es layer intensity and solar activity, indicating that higher solar
232 activity could potentially lead to a decrease in Es layer intensity. In 1984, Baggaley conducted a
233 statistical analysis of data from two stations in the southern hemisphere covering three solar
234 activity cycles. The study concluded that solar activity and the Es layer were not correlated
235 [Baggaley et al., 1984]. However, the following year, Baggaley found that Es layer intensity
236 increased with an increase in sunspot numbers [Baggaley et al., 1985].

237 To investigate the solar cycle variations in Es layer intensity in East Asia, figure 8 utilizes
238 data from five different latitude observation stations: Manzhouli, Beijing, Chongqing, Guangzhou,
239 and Haikou. The data used includes the monthly median foEs and sunspot numbers from 1998 to
240 2020, covering two complete solar cycles. This analysis aims to examine the correlation between
241 Es layer intensity and solar activity in East Asia.



242
243

Fig.8 the monthly median values of Es from 1998 to 2020



Figure 8 shows that during periods of low solar activity, such as 2006-2009 and 2017-2020, the overall foEs layer intensity is significantly higher compared to periods of low solar activity, such as 1999-2002 and 2011-2014. The Es layer in East Asia exhibits a clear negative correlation with solar activity intensity. Specifically, during years of high solar activity, the nighttime Es layer intensity is notably lower than during years of low solar activity.

In order to further investigate the correlation between Es layer intensity and solar activity cycles, the Pearson correlation coefficient was employed to calculate the correlation between daytime and nighttime monthly median foEs values and solar activity. The calculation formulas are as follows:

$$COR(X,Y) = \frac{cov(X,Y)}{\sigma_X \sigma_Y} = \frac{E(XY) - E(X)E(Y)}{\sqrt{E(X^2) - E^2(X)} \sqrt{E(Y^2) - E^2(Y)}} \quad (1)$$

where X represents the Es layer critical frequency, and Y represents the number of sunspots. The correlation calculation results between the monthly median foEs and solar activity are presented in Table 2.

Table 2 the correlation coefficient between Es layer intensity and solar activity

Index	Station name	Country	Mean correlation coefficient	Daytime correlation coefficient	Nighttime correlation coefficient
1	Beijing	China	-0.3031	-0.2665	-0.4431
2	Changchun	China	-0.0198	0.1201	-0.2665
3	Chongqing	China	-0.0133	0.0724	-0.0857
4	Guangzhou	China	-0.0629	0.0327	-0.0919
5	Haikou	China	-0.1295	0.0541	-0.1836
6	Lanzhou	China	-0.0664	0.1867	-0.2531
7	Lhasa	China	0.0259	0.1494	-0.1150
8	Manzhouli	China	-0.0970	-0.0194	-0.2780
9	Urumchi	China	-0.0510	0.0771	-0.1510
10	Qingdao	China	-0.1138	-0.0591	-0.1832
11	Sheshan	China	0.0518	0.0469	0.0605
12	Kunming	China	0.0363	0.0794	0.0113
13	Xinxiang	China	0.0858	0.1973	-0.0057
14	Suzhou	China	0.0589	0.1536	-0.0160
15	Xian	China	-0.0805	-0.0001	-0.1592
16	Wuhan	China	0.1213	0.1571	0.1682
17	Akita	Japan	-0.2905	-0.3110	-0.3664
18	Okinawa	Japan	-0.3487	-0.3007	-0.3910
19	Yamagawa	Japan	-0.3321	-0.3277	-0.3585
20	Wakkanai	Japan	0.0522	0.0847	0.0650
21	Koku	Japan	0.0553	0.1399	-0.0485
22	Average	-	-0.0657	0.0559	-0.1364

From Table 2, it is shown that there is an overall negative correlation between foEs in East Asia and sunspot numbers. At daytime, most of the stations exhibit a weak positive correlation between foEs and sunspot numbers. However, during the nighttime, almost all stations show a negative correlation between foEs and sunspot numbers.

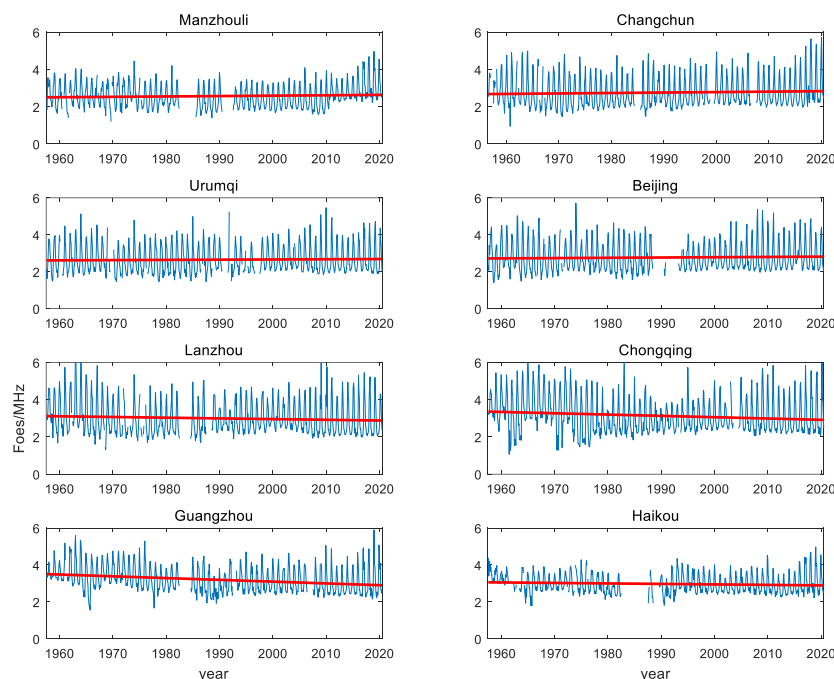


262 5. 4 Long-term variation characteristics

263 To investigate the long-term variation trends of Es layer intensity in East Asia, figure 9
264 illustrates the annual variations in monthly median foEs values at eight representative stations:
265 Manzhouli, Changchun, Urumqi, Beijing, Lanzhou, Chongqing, Haikou, and Guangzhou. The red
266 line is a linear fit of the monthly median foEs, its expression is:

$$267 f(x) = bx + a \quad (2)$$

268 where b represents the slope, and a represents the constant term.



269

270 Fig.9 the long-term variation trend of foEs monthly median

271 From figure 9, it is shown that among the eight stations: Manzhouli, Changchun, Urumqi,
272 Beijing, Lanzhou, Chongqing, Haikou, and Guangzhou, the stations with higher overall Es layer
273 intensity exhibit a decreasing trend in monthly median foEs values, while stations with lower Es
274 layer intensity show an increasing trend. Specifically, the foEs values at Manzhouli, Changchun,
275 Urumqi, Beijing, and Haikou demonstrate an upward trend, with respective positive slopes of
276 0.0002, 0.0002, 0.0001, 0.0001, and 0.0002. On the other hand, the Es layer at Lanzhou,
277 Chongqing, and Guangzhou shows a downward trend, with respective negative slopes of -0.0003,
278 -0.0006, and -0.0008. By applying the same methodology to study the long-term variation trends
279 of foEs at 13 other stations (as shown in Table 3), it was found that the Es layer intensity exhibited



a long-term decreasing trend at four stations, with negative slopes ranging from 0 to -0.0010, while it showed a long-term increasing trend at nine stations, with positive slopes ranging from 0 to 0.0024. Furthermore, the amplitude of Es layer intensity varies across different latitude stations, with the highest amplitude observed near the 30° latitude line, gradually decreasing towards lower and higher latitudes.

Table 3 long-term variation trend of Es

Index	Station name	Country	Slope	Constant term
1	Beijing	China	0.0001	2.7164
2	Changchun	China	0.0002	2.6793
3	Chongqing	China	-0.0006	3.3586
4	Guangzhou	China	-0.0008	3.5047
5	Haikou	China	0.0002	3.0587
6	Lanzhou	China	-0.0003	3.118
7	Lhasa	China	-0.0005	3.2436
8	Manzhouli	China	0.0002	2.5047
9	Urumchi	China	0.0001	2.6113
10	Qingdao	China	0.0003	3.0038
11	Sheshan	China	0.0006	3.3815
12	Kunming	China	0.0025	2.9697
13	Xinxiang	China	0.0002	3.0314
14	Suzhou	China	0.0007	3.1915
15	Xian	China	0.0024	2.9235
16	Wuhan	China	-0.0003	3.1730
17	Akita	Japan	0.0003	3.1427
18	Okinawa	Japan	0.0001	3.0874
19	Yamagawa	Japan	0.0000	3.1913
20	Wakkanai	Japan	-0.0010	3.4483
21	Koku	Japan	-0.0009	3.5679
22	Average	–	0.00017	3.091

Analysis of the monthly median foEs values at 21 stations in East Asia reveals an overall long-term increasing trend in Es layer intensity, with an average positive slope of 0.00017. Stations with higher Es layer intensity generally exhibit a long-term decreasing trend, while stations with lower Es layer intensity tend to show a long-term increasing trend. This overall pattern indicates a negative feedback characteristic. The underlying reasons for the long-term variation trends in the Es layer could potentially be associated with long-term climate variations. In our future work, we plan to conduct a more in-depth investigation specifically focused on the long-term variation trends of the Es layer.

6 Conclusion

This study utilizes over 60 years of Es layer observation data from 21 ionospheric vertical sounding stations in China and Japan to investigate in-depth the characteristics of Es layer intensity, spatial distribution, diurnal variation, seasonal variation, and long-term trends in East



298 Asia. The research findings of this study are of significant importance for exploring the causes of
299 the Es layer, analyzing the spatiotemporal distribution of Es layer intensity. The following
300 research conclusions have been obtained:

301 (1) In East Asia, the intensity of foEs during the summer months (May to August) is
302 significantly higher than in other seasons. Additionally, the intensity is notably higher around local
303 noon compared to other times of the day. Moreover, the Es layer intensity exhibits strong regional
304 variations. In general, the maximum intensity of the Es layer is located near the 30° latitude in the
305 northern Hemisphere, and weakens to lower and higher latitudes. The intensity tends to be higher
306 in lower latitudes compared to higher latitudes, and the eastern region shows slightly higher
307 intensity compared to the western region. The monthly average foEs values at all stations have a
308 maximum value above 5 MHz, with certain stations reaching even above 9 MHz, which is much
309 higher than the global average level.

310 (2) At daytime in East Asia, the center of Es layer intensity is observed in the Chongqing,
311 Guangzhou, and Suzhou areas of China. However, during the nighttime, the center of Es layer
312 intensity migrates towards the northeast, with the strongest region located in areas such as Suzhou
313 and Qingdao in China, as well as Koku and Yamagawa in Japan. The diurnal asymmetry of the Es
314 layer center may be influenced by factors such as the distribution of land and sea, as well as
315 climatic conditions.

316 (3) During the summer in East Asia, the center of Es layer intensity is located near 30°N and
317 exhibits a belt-like distribution. In the winter, the center of Es layer intensity migrates southward
318 to the Guangzhou and Haikou.

319 (4) In East Asia, the Es layer intensity in East Asia showed a negative correlation with the
320 number of sunspots overall, with diurnal inconsistency, weak positive correlation during the day
321 and negative correlation at night.

322 (5) Based on the ionosonde data from 21 stations in East Asia, the long-term variation trend
323 of Es layer intensity at different locations is different, but overall, it presents a long-term upward
324 trend and has a negative feedback characteristic. The regions with higher average Es layer
325 intensity showed a long-term downward trend, while the regions with lower average Es layer
326 intensity showed a long-term upward trend.

327

328 **Acknowledgement** Work on this study was supported by the National Natural Science Foundation
329 of China (No.42074225, 12105251, 52371354, 62201529), National Key Laboratory Foundation
330 of Electromagnetic Environment (No.6142403240302, 6142403240301), the Stable-Support
331 Scientific Project of China Research Institute of Radiowave Propagation (No.A132312217-001),
332 and Stable-Support Scientific Project of Beijing Vacuum Elec-tronics Research Institute under
333 Grant (No. A240100880). The Es layer data used in the article were all from the National Institute



334 of Information and Communications Technology (NICT) in Japan. We would like to express our
335 gratitude.
336

337 **Data Availability Statement** The Es data over China and Japan can be available at:
338 <https://github.com/zhaohaisheng22s/-Sporadic-E-Over-East-Asia/commits/Es>.
339 DOI:10.5281/zenodo.10885736.

340 Reference

- 341 Arras C., C. Jacobi, and J. Wickert (2009), Semidiurnal tidal signature in sporadic E occurrence
342 rates derived from GPS radio occultation measurements at higher midlatitudes, *Ann. Geophys.*,
343 27, 2555-2563.
- 344 Axford, W. I., The formation and vertical movement of dense ionized layers in the ionosphere [J],
345 *J. Geophys. Res.*, 1963, 68, 769.
- 346 Axford W. I., D. M. Cunnold, and L. J. Gleeson (1966), Magnetic field changes in temperate zone
347 sporadic-E layers, *Planet. Space Sci.*, 14, 909-919.
- 348 Baggaley W. J., Three solar cycles of daytime southern hemisphere Es activity [J], *J. Atmos. Terr.*
349 *Phys.*, 1984, 46, 207.
- 350 Baggaley W. J., Changes in the frequency distribution of foEs and fbEs over two solar cycles [J],
351 *Planet. Space Sci.*, 1985, 33, 457.
- 352 Christos Haldoupis, Dora Pancheva and N. J. Mitchell (2004), A study of tidal and planetary wave
353 periodicities present in midlatitude sporadic E layers, *J. Geophys. Res.*, 109,
354 doi:10.1029/2003JA010253.
- 355 Christos Haldoupis, Dora Pancheva, Terdiurnal tidelike variability in sporadic E layers (2006), *J.*
356 *Geophys. Res.*, 111, doi:10.1029/2005JA11522.
- 357 Closs, R.L. Low latitude sporadic E associated with geomagnetic activity [J], *J. Atmos. Terr. Phys.*,
358 1969: 31, 873-875.
- 359 Danilov, A. D., & Konstantinova, A. V. (2020). Long-term variations in the parameters of the
360 middle and upper atmosphere and ionosphere (review). *Geomagnetism and Aeronomy*, 60(4),
361 397-420.
- 362 Davis C. J., and K. H. Lo (2008), An enhancement of the ionospheric sporadic-E layer in response
363 to negative polarity cloud-to-ground lightning, *Geophys. Res. Lett.*, 35,
364 doi:10.1029/2007GL031909.
- 365 Didebulidze G.G., Dalakishvili G., L.Lomidze, G. Matiashevili, Formation of sporadic-E (Es)
366 layers under the influence of AGWs evolving in a horizontal shear flow [J], *J. Atmos. Sol. -Terr.*
367 *Phys.*, 2015, 136: 163-173.
- 368 Haldoupis C., Schlegel K., Characteristics of midlatitude coherent backscatter from the
369 ionospheric E region obtained with Sporadic E Scatter experiment [J], *J. Geophys. Res.*, 1996,
370 101: 13387-13397.
- 371 Haldoupis, C., D. T. Farley, K. Schlegel, Type-1 echoes from the mid-latitude E-region ionosphere
372 [J], *Ann. Geophys.*, 1997, 15, 908.
- 373 Haldoupis, C., C. Meek, N. Christakis, D. Pancheva, and A. Bourdillon, Ionogram height-time-
374 intensity observations of descending sporadic E layers at mid-latitude [J], *J. Atmos. Sol. Terr.*



- Phys., 2006, 68, 539.
- Haldoupis, C., Pancheva, D., Singer, W., Meek, C., & MacDougall, J. (2007). An explanation for the seasonal dependence of midlatitude sporadic E layers. *J. Geophys. Res.*, 112(6), 1–7.
- Helmholtz J., A multi-platform investigation of midlatitude sporadic E and its ties to E-F coupling and meteor activity [J], *Ann. Geophys.*, 2016, 34 (6): 524-541.
- Ioannidis, G., D. T. Farley, Incoherent scatter observations at Arecibo using compressed pulses [J], *Radio Sci.*, 1972, 7, 763.
- Jacobi, C., & Arras, C. (2019). Tidal wind shear observed by meteor radar and comparison with sporadic E occurrence rates based on GPS radio occultation observations. *Advances in Radio Science*, 17, 213–224.
- Kelley, M. C., D. Riggan, R. F. Pfaff, W. E. Swartz, J. F. Providakes, C. S. Huang, Large amplitude quasi-periodic fluctuations associated with a mid-latitude sporadic E layer [J], *J. Atmos. Terr. Phys.*, 1995, 57, 1165.
- Liu, Dan, Xue Kun, Xu Zheng-Wen, et al., "Characteristics of Sporadic E Layer Over and Around Qinghai-Tibet Plateau". *IEEE Geoscience and Remote Sensing Letters*, vol.19, 2022, pp.1-5, doi:10.1109/LGRS.2022.3213547.
- Macleod, M. A., T. J. Keneshea, and R. S. Narcisi (1975), Numerical modeling of a metal ion sporadic E-layer, *Radio Sci.*, 10, 371.
- Maeda J., T. Suzuki, M. Furuya, K. Heki, Imaging the midlatitude sporadic E plasma patches with a coordinated observation of space borne In SAR and GPS total electron content [J], *Geophys. Res. Lett.*, 2016, 165 (2): 275-285.
- Maksyutin, S. V., Sherstyukov, O. N. Dependence of E-sporadic layer response on solar and geomagnetic activity variations from its ion composition [J], *Adv. Space Res.*, 2005: 35, 1496–1499.
- Pezzopane, M., Pignalberi, A., & Pietrella, M. (2015). On the influence of solar activity on the mid-latitude sporadic E layer. *Journal of Space Weather and Space Climate*, 5, A31.
- Pfaff, R., M. Yamamoto, P. Marionni, H. Mori, S. Fukao, Electric field measurements above and within a sporadic-E layer [J], *Geophys. Res. Lett.*, 1998, 25, 1769.
- Pignalberi, A., Pezzopane, M., & Zuccheretti, E. (2014). Sporadic E layer at mid-latitudes: Average properties and influence of atmospheric tides. *Annales Geophysicae*, 32(11), 1427–1440.
- Qiu, L., Yamazaki, Y., Yu, T., et al., Numerical Simulations of Metallic Ion Density Perturbations in Sporadic E Layers Caused by Gravity Waves, *Earth and Space Science*, 2023, 10, e2023EA003030.
- Reddy C. A., Physical significance of the Es parameters fbEs, fEs, and foEs 2. Causes of partial reflections from Es [J], *J. Geophys. Res.*, 1968, 73 (17): 5627-5647.
- Seddon, J. C., Sporadic E as observed with rockets [M], in Smith, E., and S. Matsushita, editors, *Ionospheric Sporadic E*, P. 1962, 28.
- Sivakandan, M., Mielich, et al., Long-term variations and residual trends in the E, F, and sporadic E (Es) layer over Juliusruh, Europe. *J. Geophys. Res.*, 2023, 128, e2022JA031097.
- Smith E. K. (1957), Worldwide occurrence of sporadic E. NBS Circular 582, U. S. Gort. Printing Office, Washington. D. C.
- Smith, L. G., A sequence of rocket observations of night-time sporadic-E [J], *J. Atmos. Terr. Phys.* 1970, 32, 1247.



- 419 Swartz, W. E., G. A. Ioannidis, J. S. Shen, N. M. Brice, J. F. Rowe, Two days in the life of the
420 ionosphere over Arecibo [J], Radio Sci., 1974, 9, 769.
- 421 Tan Zixun, Huang Xinyu, Wang Shen, A preliminary investigation of ionospheric Es over
422 Wuchang [J], China. J. Atmos. Terr. Phys., 1985, 47, 959.
- 423 Tepley C. A. and J. D. Mathews (1985), An incoherent scatter radar measurement of the average
424 ion mass and temperature of a night-time sporadic layer, J. Geophys. Res. 90, 3517.
- 425 Whitehead, J. D., Production and prediction of sporadic E [J], Rev. Geophys. Space Phys., 1970, 8,
426 65.
- 427 Whitehead, J. D., Recent work on mid-latitude and equatorial sporadic E [J], J. Atmos. Terr. Phys.,
428 1989, 51, 401.
- 429 Xu, X., Luo, J., Wang, H., Liu, H., & Hu, T. (2022) Morphology of sporadic E layers derived from
430 Fengyun-3C GPS radio occultation measurements. Earth, Planets and Space, 74, 1-13.
- 431 Yamamoto, M., T. Itsuki, T. Kishimoto, R. T. Tsunoda, R. F. Pfaff, S. Fukao, Comparison of E-
432 region electric fields observed with a sounding rocket and a Doppler radar in the SEEK
433 campaign [J], Geophys. Res. Lett., 1998, 25, 1773.
- 434 Zhao, H.S. (2024a). zhaohaisheng22s/-Sporadic-E-Over-East-Asia [Dataset]. [https://github.com/
435 zhaohaisheng22s/-Sporadic-E-Over-East-Asia/commits/Es.DOI:10.5281/zenodo.10885736](https://github.com/zhaohaisheng22s/-Sporadic-E-Over-East-Asia/commits/Es.DOI:10.5281/zenodo.10885736).
- 436 Zhao, H.S. (2024b). zhaohaisheng22s/-Sporadic-E-Over-East-Asia [Software]. [https://github.com/
437 zhaohaisheng22s/-Sporadic-E-Over-East-Asia/commits/Es.DOI:10.5281/zenodo.10885736](https://github.com/zhaohaisheng22s/-Sporadic-E-Over-East-Asia/commits/Es.DOI:10.5281/zenodo.10885736).
- 438 Zhao, H. S. Z. W. Xu, Kun X. et al.(2024) Probable Controls From the Lower Layers on Sporadic
439 E Layer Over East Asia, J. Geophys. Res., 129, e2023JA032379.
- 440 Zhu F., J. Yang, Y. Qing, X. Li, Assessment and analysis of the global ionosphere maps over China
441 based on CMONOC GNSS data, Frontiers in Earth Science, 2023 10.3389/feart.2023.1095754,
442 11.
- 443 Zuo, X. M., Wan, W. X. The correlation between sporadic E-layers and solar activity [J], Chin. J.
444 Geophys., 2006, 45 (6): 759 – 765 (in Chinese).

445 **Author contributions**

447 Zhao., Feng., Liu. and Xu. wrote the main manuscript text. Xue., Wu., and Xue. prepared Figs. 1
448 – 6. Peng. and Ding prepared Figs. 7 – 9. All authors reviewed the manuscript.

449 **Competing interests**

450 Te authors declare no competing interests.